High Power K_a-Band Transmitter for Planetary Radar and Spacecraft Uplink

A. M. Bhanji, D. J. Hoppe, R. W. Hartop,
E. W. Stone, and W. A. Imbriale
Jet Propulsion Laboratory

D. Stone and M. Caplan
Varian Associates, Inc.

A proposed conceptual design of a 400 kW continuous wave (CW) K_a-band transmitter and associated microwave components to be used for planetary radar and serve as a prototype for future spacecraft uplinks is discussed. System requirements for such a transmitter are presented. Performance of the proposed high-power millimeter wave tube, the gyroklystron, is discussed. Parameters of the proposed power amplifier, beam supply, and monitor and control devices are also presented. Microwave transmission line components consisting of signal monitoring devices, signal filtering devices, and an overmoded corrugated feed are discussed. Finally, an assessment of the state of the art technology to meet the system requirements is given and possible areas of difficulty are summarized.

I. Introduction

Due to present user crowding of the S- and X-band microwave spectrums assigned to space exploration and to anticipated new user requirements that can be met by higher frequencies, the Jet Propulsion Laboratory has initiated a design and development program for a next generation K_a-band (34 GHz) continuous-wave (CW) transmitter that will first be used for planetary radar applications where shorter wavelength offers increased resolution of targets and improved ranging capabilities. The technology will be transferable to uplink communication with future spacecraft. The scientific value of a K_a-band radar can be assessed by breaking the criteria down into those that rely on the shorter wavelength to give new information and those that require greater two-way antenna gain. The shorter wavelength will be especially valuable in the investigation of Jupiter's moons, the rings of Saturn, and the detection of rain in the upper atmosphere of Venus. The number of detectable asteroids in a ten-year span will be enhanced by a factor of 10 due to higher antenna gain.

The experimental transmitter will be installed on the 64 meter Cassegrain antenna at Goldstone, California (Fig. 1) (Ref. 1), which is equipped with a rotatable, asymmetric hyperboloidal subreflector that permits the use of multiple feed systems at the Cassegrain focus. The subreflector can be precision indexed to a fixed number of positions that will allow each feed to properly illuminate the main reflector. The 64-meter antennas were designed in the early 1960's for S-band operation and subsequent modifications have resulted

in some 60 percent aperture efficiency at 8.5 GHz (Ref. 1). A block diagram of the existing transmitters and the proposed K_a-band transmitter to be installed on the 64 meter antenna is shown in Fig. 2. To achieve a reasonable antenna efficiency at the 34 GHz band, an upgrade of the antenna dish structure and surface panel accuracy is required and is part of a planned implementation project to extend the 64-meter diameter dish to 70 meters and incorporate shaped surfaces. The increased antenna diameter and shorter wavelength are expected to provide an antenna gain of 84 dB, and with the proposed 400 kW CW transmitter, the K_a-band radar system will have an effective radiated power of about 100 trillion watts.

Using an assessment of the state-of-the-art technology, this article will present a proposed conceptual design and calculated performances of a 400 kW CW K_a-band transmitter including overmoded transmission line components (e.g., taper, coupler and a mode filter) and an overmoded antenna feed system.

II. Transmitter System Requirements

The transmitters for radar astronomy systems differ from conventional radar systems in that they require a high average power, rather than high peak power, over the bandwidth required to handle the transmitted signal (Ref. 2). It is also important that these transmitters be coherent in order to determine the phase relationships of the returned signals, and they must have very high phase stability if measurements are to be made over long periods of time. The transmitter must also be capable of modulation by a variety of pulse programs while maintaining the phase and amplitude fidelity and pulse to pulse stability required for pulse compression systems incorporated in the radar.

The performance of a pulse compression system (Ref. 3) depends upon the transmitter stability, phase response, and amplitude response to preclude the creation of large time sidelobes (spurious amplitude responses on either side of the main compressed signal). By control of these characteristics and the use of weighting techniques, the compressed pulse system time sidelobes can be kept below -30 dB. If the transmitter phase pushing is not to degrade this level, spurious sidelobes due to the transmitter alone must be kept below -40 dB. The sidelobe level (Ref. 3) is given by:

$$SL = 20 \log \frac{\Delta P}{2} \qquad (1)$$

where ΔP is the peak phase ripple during the transmitter pulse. For a subsystem time sidelobe level of -40 dB, $\Delta P = 1.15^\circ$.

The requirements for such a radar transmitter are then:

(1) High power

(2) Low incidental phase modulation (jitter)

(3) Phase stability

(4) Low incidental amplitude modulation

(5) Amplitude stability

(6) Frequency stability

(7) Bandwidth

(8) Low harmonics

(9) Low noise

(10) Phase modulation (phase code pulse compression (PN))

(11) Frequency shift keying (FSK)

(12) Linear capability

The above requirements illustrate that high power alone will not provide the desired CW radar transmitter capabilities. If this were the case, it might be more easily obtained with an oscillator instead of an amplifier. Besides the appeal of having dynamic control of amplitude and phase, the appeal for using an amplifier is that it eliminates the need for phase locking an oscillator to a control signal. The control signal itself could, after amplification, be the transmitted signal.

Based on the above requirements, the K_a-band radar transmitter specifications are given in Table 1.

III. The Transmitter

As shown in Fig. 3, the transmitter will include an existing power supply that converts 2400 V, 3 phase, 60 Hz line voltage to direct current at up to 90 kV with a power limitation of 1.1 MW for the gyroklystron (to be described later) amplifier beam. The frequency synthesizer and the exciter will provide an input signal to this 400 kW gyroklystron amplifier which will provide approximately a 50 dB power gain (goal). The automated transmitter control will furnish monitoring and control of all functions, while some 40 protective devices (interlocks) will prevent damage to equipment by removing voltage and in some cases drive power in event of a malfunction. The liquid to air 1.5 MW heat exchanger will be used to cool the amplifier, the power supply, various auxiliaries to the transmitter, and microwave components of the transmission line.

A. High Power Millimeter Amplifier Tube

The gyroklystron is a potential candidate.

1. Requirements background. The requirements of high power, high gain, ease of modulation and an output spectrum free from spurious signals and noise makes a klystron linear beam tube the natural choice for radar. However, at K_a-band frequencies, an examination of commercially available linear tubes shows there are no conventional klystrons, twystrons, or TWTs that can meet the specifications given in Table 2 (these specifications are derived from the K_a-band radar transmitter specifications given in Table 1). These conventional microwave tubes cannot be scaled to 34 GHz (K_a-band) and maintain high efficiency and high power because of heat transfer problems in the relatively small electron interaction volume. The result is that less conventional devices operating in higher order modes (thus larger in circuit area and dissipation capability) become attractive, and the usual $P = K/f^2$ (Ref. 4) scaling condition can be ignored.

The *gyrotron* (Ref. 5) or cyclotron resonance maser is such a device. The interaction mechanism responsible for microwave amplification in the so called fastwave device is azimuthal phase bunching due to the dependence of the electron cyclotron frequency on the relativistic electron mass and magnetic coupling to RF fields in the cavity/waveguide close to cut-off. Experimental research in this field has produced some exciting and impressive powers and efficiencies (Ref. 6).

However, these oscillators are not suitable for all applications (the primary use is for plasma heating) because they are essentially fixed frequency devices. There is considerable interest in gyroamplifiers for radar systems and satellite communications.

Early gyro-TWT amplifier development was promising but results did not greatly surpass the performance of conventional TWTs. The reason was that since the gyro-amplifier has a much longer interaction region than the gyro-oscillator, the destruction of phase bunching due to velocity spread in the electron beam is greater. However, improved gun design with a small velocity spread has led to some significant results. High efficiencies (25%) have been demonstrated in an experimental C-band gyroTWT at Varian Associates (Refs. 7 and 8). More recently, Varian has operated a 94 GHz gyroTWT with a 30 dB gain, 2% bandwidth, output power larger than 20 kW and an efficiency of 8%. The mode of operation is TE_{11}. There is also ongoing work at the Naval Research Laboratory (NRL) in Washington, D.C., to develop a wide bandwidth (10%) gyro-TWT (Ref. 9).

There continues to be interest in developing a gyroklystron amplifier consisting of resonant gyro-oscillator type cavities separated by drift tubes. An experimental gyroklystron is now being assembled at NRL with the following objectives (Ref. 10): frequency 4.5 GHz (the experiment is being performed at C-band due to the availability of a Magnetron Injection Gun (MIG) suitable for this frequency range); small signal gain >40 dB; efficiency >35%; output power >100 kW; and a bandwidth of about 1%. Measurements will be made to determine such characteristics as efficiency, gain, bandwidth as a function of magnetic field, and cavity tuning. An earlier ORNL K_a-band gyroklystron (Ref. 11) built at Varian did not meet design goals of power and efficiency and it was recognized that the principal difficulty with the 28 GHz gyroklystron was oscillation in the drift tubes, which were capable of supporting propogating modes because the buncher cavities themselves were designed to operate in the overmoded TE_{011} mode. However, a great deal of practical engineering information has been learned from this first gyroklystron work, and with the inclusion of Varian's design study of a gyroklystron for the NASA Lewis Research Center (Ref. 12) and work at NRL (described above), the gyroklystron appears to be the natural choice for a JPL K_a-band transmitter that will meet the tube specifications listed in Table 2 for high gain, high efficiency, high power, and narrow bandwidth. A paper design of the proposed 34 GHz gyroklystron and its characterization in terms of efficiency, instantaneous bandwidth, small signal and saturated gain, AM and PM sensitivity to operating parameters, spectral purity, phase stability and noise figure follows.

2. Paper design of JPL gyroklystron. The overall design considerations for gyroklystrons resemble in many ways the design procedures for conventional klystron amplifiers, even though the gain mechanism involves a beam interaction with cyclotron waves rather than space-charge waves. Caplan (Ref. 13) has shown that the same equivalent circuit used for many years in describing klystrons can be used to describe gyroklystrons if transadmittance, beam loaded Q's, and beam reactance are appropriately redefined for a gyroklystron.

The basic design approach is shown in Fig. 4. A Pierce gun produces a beam which is injected into a wiggler field to impart the rotational energy to a solid beam and then adiabatically compressed to the circuit. The circuit consists of 3 buncher cavities operating in the TE_{111} mode and an output cavity in the TE_{121} mode. A small, tapered transition is made to 0.787 in. diameter, at which point there exists a 7-inch-long mode converter to transform the TE_{12} circularly polarized mode to the TE_{11} circularly polarized output mode. The waveguide is then tapered optimally to the collector region where the spent beam is deposited. The down taper region then leads to a face-cooled double disc 2.5-inch diameter window.

The gyroklystron circuit consists of a number of cylindrical cavities operating in the transverse electric mode interconnected by cut-off drift tubes through which the rotating electron beam passes. As in conventional klystrons, the input

cavities and drift tubes serve to prebunch the beam while the actual rf energy interaction occurs in the output cavity, which in this case is an open irregular resonator. Designing a circuit consists of choosing the cavity lengths, drift tube lengths, and cavity Q's such that when an electron beam of desired voltage, current and rotational energy is made to pass through the circuit, the required gain, bandwidth and efficiency will be obtained, while at the same time circuit stability against spontaneous oscillations is maintained.

Because of power handling considerations and mode integrity, the rf power cannot be extracted conventionally through a coupling hole at right angles to the device, but must travel in line with the beam through an up taper and collector region.

As stated earlier, gyrotron-type devices can operate at high power and high frequencies; however, this introduces the problem of suppressing other unwanted modes in the cavity whose cutoff frequencies are close to the desired mode. Since the desired output mode in this case is TE_{11} circularly polarized, which is the dominant lowest order mode, the choice of this operating mode for the gyroklystron is desirable since it rules out mode competition. However, the requirement of 400 kW CW at 34 GHz demands a higher order mode in the output cavity if the power densities dissipated on the cavity walls are to be less than 1 kW/cm^2 (proven standard heat transfer technology at this time). Since there is no energy exchange in the input buncher cavities, these can operate in the TE_{111} dominant mode, thus eliminating the problem of unwanted interaction in the drift tubes. One can now have an overmoded output cavity, provided the symmetry of the output cavity mode is compatible with the bunching pattern imposed on the beam from the TE_{111} mode. This then requires the output cavity to be of the TE_{1n1} type; i.e., the azimuthal index 1 must be the same as that for TE_{111}. The power dissipation in such a cavity is given by Ref. 14 as:

$$P(W/cm^2) = 4.8377 \times 10^{-5} \frac{f_0^{5/2} P_0 Q_{ext}}{K_{mn}2 (L/\lambda_0) \left(1 - \frac{m^2}{K_{mn}2}\right)} . \quad (2)$$

where

f_0 = frequency (GHz)

P_0 = output power (kilowatts)

Q_{ext} = external Q of output cavity

K_{mn} = transverse mode number for TE_{mn} mode

L/λ_0 = cavity length in units of free space wavelengths

The lowest order mode that will satisfy the criterion that $P < 1$ kW/cm^2 is the TE_{121} mode with $Q_{ext} \leq 400$ (a requirement in order to achieve bandwidth of 0.1%) and $(L/\lambda_0) \geq 3$ (for efficiency).

The overall stability of the gyroklystron amplifier (against the propensity to become an oscillator) is ensured by using sufficiently short cavities and low enough cavity Q's such that the threshold currents required for each cavity to self-oscillate are above the operating current. A sufficient number of cavities are then used to achieve the required gain of 50 dB.

As in all gyrotrons, one is required to create an electron beam with 70-80% of its energy in rotational motion. Two methods used for producing such a beam are the MIG and the Pierce gun/wiggler configuration. The wiggler configuration has not yet been used in oscillators as has the MIG, and thus has not yet had the opportunity to demonstrate, in a direct comparison, the capability of generating beams of a quality (low velocity spread) which equal or surpass MIG beam quality. One advantage of using the wiggler is that standard Pierce gun technology can be used, which ensures operation with a space charge limited beam (resulting in low noise, an important requirement for radar and communications tubes).

With the output cavity operating in the TE_{121} mode, power must be converted back into the desired TE_{11} mode and run into an overmoded waveguide in order for the output window and collector to handle the CW power requirement. A symmetric ripple wall mode converter will be used to convert TE_{12} to TE_{11} with $> 99\%$ conversion efficiency. The collector will have to be at least 4 inches in diameter for reliable power handling capability during operation with 1 MW CW of beam power. This requires tapering up the waveguide to 4 inches and then back down to the "standard" 2-1/2-inch output window. Non-linear gaussian tapers which can maintain 95% mode purity in these tapered sections will be used. A mode filter will be required in the external transmission line to remove this last 5% power in undesired modes, which consist mainly of the TE_{12}, TE_{13}, as well as TM_{11}, TM_{12}, TM_{13}, and TM_{14} modes. The next section will cover the calculated performances of a few of the tube components and their parameters, including operating characteristics.

3. Calculated performances and operating characteristics.

a. Circuit design. The calculated performance of the circuit design consists of a computer-simulated analysis of a large number of possible circuit configurations, using the small signal gyroklystron gain program for gyroklystron amplifiers developed at Varian by Caplan (Ref. 13) and a large signal efficiency program.

For a given set of input parameters, the small signal gain program calculates gain, beam-loaded Q's, beam reactance, transadmittances, cavity amplitudes, and phases, all as a function of frequency and magnetic field. These results are then used as inputs to a large signal code, which integrates a large number of particle trajectories through electric fields (calculated in the small signal code) to determine the amount of energy lost by the beam. This code uses an iteration procedure to determine saturated field amplitude in the last cavity. It is assumed that the field amplitudes and phases in the input cavities calculated from linear theory are valid even at saturation, since these cavities only serve to prebunch with little energy extraction. For a final check on the design and performance, an eleborate particle simulation code that uses up to 5000 particles will be used. Subtle effects such as beam loading on the mode structure can be studied and very accurate estimates of the effects of velocity spread on efficiency can be calculated.

A four cavity gyroklystron circuit design that meets the JPL specifications is given in Table 3. Figures 5 and 6 show calculated results of gain vs. frequency, and power out vs. power in (indicating a saturated output of 465 kW and 46.5% efficiency), respectively, for this gyroklystron. These calculations were based on the beam having zero axial velocity spread (cold beam). It is estimated that with a velocity spread (hot beam) of 5%, the efficiency would drop to 35%.

As stated earlier, a gyroklystron can be described by the same type of equivalent circuit as a regular klystron. The major difference is that the circuit elements such as beam loaded Q and transadmittance can have a strong dependence on magnetic field and frequency when compared with a conventional klystron. A small change in magnetic field can result in large changes in gain and efficiency. Figure 7 shows efficiency vs magnetic field for the above gyroklystron.

b. Mode converter. The power emitted from the output cavity will be in the TE_{12} mode, and therefore a mode converter must be designed to convert it to the desired TE_{11} mode. A relatively simple cylindrically symmetric mode converter (Ref. 15), which consists of a section of waveguide having a sinusoidal variation of the wall radius, $a(z)$, with distance, can be designed. For the converter, $a(z) = a_o + \delta_a \sin(2\pi z/\lambda_b)$, where a_o is the average wall radius, λ_b is the wavelength of the ripples, and δ_a is the amount of maximum wall perturbation. Mode conversion is accomplished by choosing the ripple wavelength equal to the beat wavelength between the TE_{11} and TE_{12} mode, $2/\lambda_b = 2/\lambda_{11} - 2/\lambda_{12}$. The optimum converter length is given approximately as $L_c = 0.638\lambda_b/(\delta_a/a_o)$. For a_o = 1 cm, which is about 25% above cutoff of the TE_{121} cavity, the beat wavelength is equal to 2.915 cm; choosing a ripple amplitude of 0.10626 cm makes the optimum converter length 6.9 inches. This design was checked using Varian's computer code which solves 20 coupled telegrapher's equations inside a waveguide of arbitrary wall profile. The code solves for the mode conversion occurring from the TE_{12} mode to all other modes with the same azimuthal symmetry, m = 1, which are the only conversions allowed in a symmetric converter. Figure 8 shows the calculated performance of such a converter. As expected, almost all power is converted to the desired TE_{11} mode, with the worst offender being TM_{12} at -23 dB (1/2%). Table 4 shows the calculated amount of power in each of the spurious modes at the end of the converter.

c. Beam collector. The collector has to satisfy two constraints which work directly against each other. It must dissipate high beam power at levels of no more than 1 kW/cm^2. This means the collector must be as large as possible, but at the same time it is desirable to keep the diameter of the output waveguide configuration (of which the collector is a part) as small as possible to ensure mode purity. Spurious modes will also be generated in the collector since the collector will contain tapers. For example, the up-taper will connect the 1" diameter waveguide at the end of the mode converter to the 4" diameter waveguide in the beam deposition region. Using non-linear taper designs, and the analysis by Sporleder and Unger (Ref. 16), a 4" taper design (optimized for a 60 GHz gyrotron) was examined for its mode conversion properties when used for the TE_{11} mode. A Varian program based on Sporleder and Unger's coupled mode theory, which solves for simultaneous coupling of the TE_{11} mode to as many TE_{1n} and TM_{1n} modes as are necessary to model the problem, was used. Figure 9 shows the total spurious mode level for all TE_{1n} modes versus axial distance. The taper described in Fig. 9 was not optimized to discriminate against TM_{1n} modes. With TM modes included in calculation, 10% of power was converted to TM_{11}. Further effort is being made to optimize the taper sections for the JPL gyroklystron to avoid conversion to TM modes.

d. The CW output window. The primary design approach for the CW output window is a double ceramic disc face-cooled with fluorocarbon liquid as shown in Fig. 10. Performance for a window of this type has already been demonstrated at K_a-band at power levels well above the 200 kW minimum (340 kW CW at 28 GHz). At 60 GHz the double disc concept has also proven capable of 200 kW CW (Ref. 17). These data prove that a 200 kW 34 GHz double disc window is feasible and indicate that a 400 kW CW 34 GHz double disc window can be designed to operate successfully.

Initial calculations for the 400 kW CW 34 GHz window, a design with sapphire window discs, offers ample bandwidth

(over 1.5 GHz for a Voltage Standing Wave Ratio (VSWR) ≤ 1.5:1 as shown in Fig. 11). Finite element heat transfer calculations predict a worst case peak temperature of 65.1°C at the center of the window face on the vacuum side. The resulting thermal stresses in the window material are well within conservative estimates of loads which cause sapphire breakage.

Having described the calculated performance of some of the components of the proposed gyroklystron, it is next appropriate to characterize the tube in terms of noise figure and AM and PM sensitivities.

e. Noise figure. The noise figure for the proposed gyroklystron configuration is calculated using the standard shot noise expression (Ref. 18).

$$P_{\text{noise}}\,(\text{dB}) = 10 \log \left[\frac{2eI_o\,\Delta f\,\Gamma^2\,\beta^2\,G_{ss}\left(\frac{R_{\text{shunt}}}{Q_1}\right)Q_1}{P_{\text{out}}} \right] \quad (3)$$

where e is the electron charge, I_o is the beam current, Δf is the noise bandwidth, P_{out} is the output power, G_{ss} is the small signal gain, R_{shunt} is the shunt impedance of the first cavity, and Q_1 is the first cavity Q.

This expression has been found to be accurate for klystron amplifiers (Ref. 19) and it applies equally well to gyroklystrons. However, the parameters for the coupling cavity (β^2) and first cavity shunt impedance (R_{shunt}) must reflect the properties of the gyroklystron cavity design. Using the values, $R_{\text{shunt}}/Q_1 = 1433\Omega$, $Q_1 = 300$, $G_{ss} = 57$ dB, $\beta^2 = 0.9$, $\Gamma^2 = 2.39 \times 10^{-6}$, $I_o = 12.5$A, $\Delta f = 1$ MHz, and $P_{\text{out}} = 200$ kW, gives $P_{\text{noise}} = -110.3$ dB/MHz, which meets the tube specifications given in Table 2.

f. AM and PM sensitivities. In order to calculate AM and PM sensitivities with respect to various operating parameters of the proposed gyroklystron, responses of each section of the tube must be included in the calculation. For example, to determine the AM and PM sensitivity of the tube due to variation in the gun coil current, the following individual sensitivity factors must be multiplied together to provide overall sensitivity.

$$\left(\frac{\text{gauss}}{\text{amps}}\right)_{\substack{\text{gun coil}\\ \text{variation}}} \times \left(\frac{\%}{\text{gauss}}\right)_{\substack{\text{Pierce}\\ \text{gun}\\ \text{scalloping}}} \times \left(\frac{\%}{\%}\right)_{\substack{\text{wiggler}\\ \text{velocity}\\ \text{spread}}} \times \left(\frac{\%}{\%}\right)_{\substack{\text{adiabatic}\\ \text{compression}}} \times \left(\frac{\text{dB, deg}}{\%\ \%}\right)_{\substack{\text{circuit}\\ \text{sensitivity}}}$$

$$= \left(\frac{\text{dB}}{\text{amps}}, \frac{\text{deg}}{\text{amps}}\right)_{\substack{\text{Tube}\\ \text{sensitivity}}} \quad (4)$$

Tables 5 and 6 give very preliminary calculations of AM and PM pushing factors, respectively, with respect to cathode voltage, magnet coil current, and load VSWR, etc.

The results of a preliminary calculation of phase linearity are given in Fig. 5. Some parameters are yet to be calculated and will be given in a later report.

B. Power Amplifier

A functional block diagram of the proposed transmitter power amplifier is shown in Fig. 12. The power amplifier will be driven to a 400 kW CW output by a helix traveling wave tube preamplifier. Such a driver power preamplifier tube at 30 GHz with 40W output has been developed at the Nippon Electronics Corporation (NEC) in Japan (Ref. 20). The output of the preamplifier will be monitored through a 50 dB coupler and will be isolated from the gyroklystron power amplifier input by means of a circulator and attenuator. This is necessary to maintain the amplitude and phase response of the system over the 340 MHz bandwidth of the preamplifier, as the match of the gyroklystron power amplifier input will vary considerably over this band. In addition, the circulator-plus-attenuator must have a high (50 kW peak, 10 kW average) rating for reflected power in order to survive spurious emission from the gyroklystron input port which occurs when the gyroklystron is first installed and tuned up in the transmitter. The input of the preamplifier (TWTA) will be driven by an exciter which is required to generate the 34 GHz frequency and ±10 MHz phase modulation bandwidth for the radar. This exciter may have a switched output of 44 MHz which would then drive a multiplier (x 772) to obtain 34 GHz. The inexorable consequence of this frequency multiplication is the multiplication of phase modulation by $(772)^2$ (Ref. 21). This implies that the degradation by the multiplier has to be kept near the theoretical minimum. The specifications of such a multiplier will be very stringent, and none of these multipliers have been built yet.

Another area of crucial interest is the guiding magnet. This device is a solenoid which surrounds the interaction volume and keeps the electron beam focused in the tube length before the collector. A control of better than 1% must be exercised to maintain high efficiency (as shown in

Fig. 7) and, typically, a range of 600-700 A and 30-60 V would be required to maintain a 12.5 kG field if a water-cooled copper solenoid were to be used. At present, it has not been determined whether the solenoid should be a conventional magnet composed of a copper conductor with a hollow water channel for cooling, or a superconducting magnet composed of Nb_3S_n embedded in a copper matrix. Since power dissipation will be an important parameter, if the superconducting solenoid does not give a factor of 1000 to 1 lower power dissipation than that achievable at room temperature, its advantage over the conventional copper magnet is doubtful. Another factor to be considered is that for every watt of transfer in the cooled superconducting structure, about 400 watts of power must be supplied at the refrigeration system input (Ref. 22). The third factor to consider are the constraints on the design of the superconducting solenoid due to the fact that the magnet (and the gyroklystron) will have to tilt through 75° from zenith and rotate through 360° azimuth when tilted. However, tiltable superconducting designs have already been studied for other gyro device applications (Ref. 23). The main advantage of a superconducting magnet, besides its being small in size and weight, is that it provides a virtually ripple-free magnetic field profile in the gun, wiggler, and circuit. This ripple-free profile is essential in order to keep PM distortion down, as can be seen from Table 6.

The gyroklystron output, at 400 kW CW, will be fed via a waveguide arc detector, a forward and reverse power overmoded waveguide coupler, and a mode filter to an overmoded feed system for final antenna illumination. This overmoded transmission line with microwave components and an overmoded feed system is discussed later.

The gyroklystron body, collector, filaments, waveguide components, etc., will be cooled by distilled and deionized water, which in turn will be cooled by ambient air in an external existing heat exchanger. The details of the gyroklystron beam supply are described in the following paragraph.

C. Beam Supply

A block diagram of the existing beam supply is shown in Fig. 13. Power at 12,600 V, 3 phase, and 60 cycles per second is supplied to separate substations from a commercial line which is underground for the last mile. The 2400 V substation supplies the main motor generator only, while all auxiliaries are supplied from a 480 V substation. The output of the main motor generator at 400 Hz is stepped up in voltage in the transformer, rectified, and delivered to the load through a filter, crowbar, and series-limiter resistor at voltages adjustable up to 90 kV and 1.1 MW maximum. The output ripple under full load is less than 0.05%.

The use of a frequency converter (such as the motor generator) might seem unnecessary but actually provides worthwhile technical and economic advantages. It isolates the power line from a crowbar of the dc supply and greatly simplifies line protection problems. It also isolates the supply from short duration line voltage fluctuations and transients due to the large inertia of its rotating components. The change from 60 to 400 Hz reduces all transformer and filter sizes and costs.

The beam supply is required to provide 80 kV between the gyroklystron collector and cathode at a beam current of 12.5 amps during the long radar pulse (up to 4 hours).

Referring to Eq. (1) and Table 6, the intra-pulse ripple on the supply must be kept below 0.18% peak (144 volts peak for typical 80 KV for the gyroklystron) for pulse compression time sidelobes of -40 dB.

The ability of the beam supply to remain ripple-free during the long pulse depends upon the quality of the storage capacitor and wiring inductance between the tube and supply. It is also desirable to keep the storage capacitor as small as possible so as to limit the energy available to discharge in the tube during an arc.

The supply must be capable of withstanding the stress imposed on it when an arc occurs in the gyroklystron. The resultant firing of the crowbar will produce a peak current of 20,000 amps and a peak power of 1600 MW.

D. Monitor and Control

A transmitter monitor and control group (which will be comprised of the power amplifier monitor and control assembly in the antenna, transmitter control cabinet on the ground, and remote radar control in the operations room) will contain the control facilities and indicators necessary for an automated interface with the transmitter. This group will monitor the transmitter circuits and signals to determine the operational status. There will be some 20 major interlocks associated with the gyroklystron output stage alone and the status of each will be indicated. A memory circuit will be incorporated to "hold" an indication of intermittent fault to assist in fault diagnostics. Built in test equipment (BITE) and fault isolation test points will be provided for ease of maintenance and serviceability.

Faults demanding immediate protection such as a gyroklystron arc will result in the firing of the crowbar and the power supply will be shut down. The control unit will be programmed to run the system up again after a short delay, the length of which will depend upon the gas pressure within the gyroklystron envelope. This will be monitored by an ion pump. If the fault persists, the transmitter will remain in the

run down condition with appropriate faults indicated. A fault such as loss of coolant will cause the beam supply to be turned off, while a fault such as a waveguide arc will cause the drive and beam to be removed.

These monitoring and control assemblies will be shielded against both magnetic and electrostatic fields so that transients associated with the high power transmitter operation do not interfere with interlock logic circuit functions, and noise immunity will be achieved through the use of high threshold logic. The interlock functions will be connected via balanced lines and optical isolators as appropriate, to ensure reliable operation even in the presence of the large discharge currents associated with crowbar firing.

The supervision of this monitor and control group will be microprocessor based, which will allow the monitoring and displaying of a wide range of parameters, together with automatic run up and run down sequencing during normal operation and under fault conditions. The automatic shut down system will continuously monitor critical parameters and will take executive action under fault conditions that could lead to gyroklystron damage. A precision multiplexed analog–digital converter will monitor a large number of analog system parameters, all of which will be displayed on front panel meters. A serial interface (RS 232) will be provided to permit full monitoring and control of the transmitter including data logging via a remote radar control terminal in the operations room.

IV. Transmission Line System (Microwave Components)

In this section a description of the components comprising the transmission system will be given. A preliminary layout for an overmoded 400 kW CW transmission system is shown in Fig. 14. The components in the transmission system consist of signal monitoring devices, signal filtering devices and a circular waveguide taper. The monitoring devices include a waveguide arc detector, forward and reverse mode selective directional couplers, polarization monitoring and harmonic content monitoring devices. The only filtering device is the TE_{11} mode filter which serves three purposes: filtering unwanted spurious modes, ensuring the circularity of the TE_{11} mode, and filtering high harmonics.

The first component in the system immediately following the gyroklystron output window is a waveguide arc detector. This device allows the beam power and drive power to be disconnected should an arc be detected in the output waveguide, thus preventing permanent damage to the tube. Circular waveguide arc detectors of 2.5 inch diameter are designed routinely for use with 28 GHz and 60 GHz 200 kW CW gyrotrons.

Although the preferred diameter for the double disc window at the gyroklystron is 2.5", there are great advantages in using a smaller waveguide diameter for the remainder of the transmission system. Aside from the fact that fewer spurious modes can propagate at the smaller diameter, the overall lengths of the directional couplers and mode filter are strongly dependent on the waveguide diameter. Mode selective directional couplers are generally of the phase velocity type, obtaining mode discrimination from the fact that different modes propagate with different phase velocities. These differences in phase velocity increase with decreasing waveguide diameter. Similarly, the mode filter's operation is based upon the fact that different modes require different surface currents on the waveguide wall. These differences also increase with decreasing waveguide diameter.

For the reasons mentioned above, a smaller diameter of 1.75" is being considered for the transmission system. This diameter still allows for relatively low loss transmission and will handle the high CW power, but reduces the overall directional coupler and mode filter length. The allowable length for the gyroklystron and transmission system is determined by the height of the feed cone, which is approximately 16 feet. Additional length may be available, depending on the antenna feed length, since the phase center of the feed is located three feet above the top of the feed cone. The dimension of 1.75" is also preferred since this diameter is the approximate aperture diameter required for most efficiently illuminating the Cassegrain antenna. At present all of the JPL feeds have identical radiation patterns, and the scaled aperture diameter for 34 GHz is 1.75". Therefore with a 1.75" transmission system no flared horn is required. The feed will be discussed in more detail in a later section.

A circular waveguide taper will therefore be included as the next component in the transmission system, tapering down from the 2.5" window diameter to the preferred diameter of 1.75". A nonlinear taper, of the type described earlier, will be optimized for minimum length while the total spurious mode level will be kept below −15 dBc. The spurious mode most strongly coupled to the TE_{11} mode is the TM_{11} mode, which is, unfortunately, one of the most difficult modes to filter out.

Directional couplers are required for monitoring the forward and reflected TE_{11} wave. The couplers must not only be capable of distinguishing between forward and reverse traveling TE_{11} waves, but they must also be able to distinguish between the TE_{11} mode and each of the spurious modes. That is, the couplers must be both directive and mode selective. Mode selective directional couplers can be designed using the coupled transmission line analysis of Miller (Ref. 24). The physical layout of a dual mode selective directional coupler is

shown in Fig. 15. Here the overmoded circular waveguide is coupled to a rectangular waveguide operating in the dominant mode.

If the phase velocities of the desired TE_{11} mode in the circular waveguide and the dominant mode in the rectangular coupling guide are chosen to be equal, then the forward mode discrimination is defined as the forward coupled power for the desired mode divided by the forward coupled power for the spurious mode. For the n^{th} spurious mode, this ratio is given by

$$\text{Discrimination} = 20 \log \frac{C_o \int_{-L/2}^{L/2} \Phi(x)\, dx}{C_n \int_{-L/2}^{L/2} \Phi(x)\, e^{i\Delta\beta x}\, dx} \quad (4)$$

where L is the overall coupling length,

C_o is the coupling coefficient for the TE_{11} mode,

C_n is the coupling coefficient for the n^{th} spurious mode,

$\Phi(x)$ is the coupling function,

$\Delta\beta$ equals $\beta_o - \beta_n$,

β_o is the phase constant of the desired mode, and

β_n is the phase constant of the n^{th} spurious mode.

Discrimination between forward and reverse traveling waves may be evaluated using an equivalent formula by appropriately redefining the quantity $\Delta\beta$.

Recently, mode selective couplers of the TE_{on} type have been designed and built by Felch et al. (Ref. 25), and Janzen and Stickel (Ref. 26). A coupler design using uniformly spaced round coupling holes with an axially tapered coupling profile capable of providing a coupling factor of -60 dB in the forward direction, -40 dB in the reverse direction, and 40 dB directivity will be investigated. Mode discrimination between the TE_{11} mode and each of the TE_{1n} and TM_{1n} modes will be greater than 40 dB.

Polarization monitoring devices may be included before and after the mode filter, providing a measurement of the ellipticity of the TE_{11} mode in the circular waveguide. The preferred configuration for the polarization monitor is a section of straight waveguide with two coupling pinholes located 90° apart about the waveguide center line. A combining bridge consisting of a hybrid T, phase shifter, attenuator, and crystal detector in a standard WR-28 waveguide will then be capable of determining the ellipticity of the output signal.

The final component of the transmission system to be considered is the TE_{11} mode filter. The present estimate is that the worst case total spurious mode level at the output of the gyroklystron (including realistic effects of slight misalignments of the tube and component assemblies, insulating gaps in the tube output waveguide, etc., over the range of operating parameters) will be approximately -15 dBc. The exact distribution of the spurious mode power must be determined by actual measurements on the gyroklystron itself; however, the calculations from the paper design indicate that the primary spurious modes will be the TM_{11}, TE_{12}, and TM_{12} modes. Since the exact phase and amplitude distribution of these spurious modes is unknown, the TE_{11} mode filter will be included in order to provide a well defined signal at the input to the overmoded feed. An attempt will be made to design a mode filter capable of filtering each of the spurious modes to a level of -30 dBc. The mode filter will be of the helically loaded type, as described by Morgan and Young (Ref. 27). A schematic diagram of the TE_{11} mode filter is shown in Fig. 16. In this type of mode filter the smooth waveguide wall is replaced by a conducting helical winding which is surrounded by a lossy dielectric. The pitch of the helix is chosen so that the surface currents of the desired mode, in our case the TE_{11} RCP mode, follow the windings. Spurious modes, including the orthogonal TE_{11} polarization, suffer attenuation when passing through the filter. Elliptically polarized TE_{11} signals, which can be decomposed into TE_{11} RCP and LCP components, will therefore be purified by removing the LCP component and retaining only the desired RCP component. The amount of attenuation for a particular spurious mode depends upon the conductivity of the lossy jacket and the direction of the surface currents for the specific mode. Surface currents for the TE_{11} mode tend to become more longitudinal as the waveguide diameter increases and TM modes have purely longitudinal currents for any waveguide diameter. In order to obtain significant attenuation for TM modes, it is advisable to use as small a guide diameter as possible. Therefore the length of the filter section is critically dependent on the required attenuation for the TM_{11} mode. Tolerances on the helix pitch are determined by allowable attenuation for the TE_{11} RCP mode. The preferred filter configuration consists of a copper helix, bonded to a beryllia cylinder, backed by a water jacket.

Finally, requirements on the tolerances for alignment of the tube, waveguide components, and feed necessary to preserve the spurious mode level will be determined using the formulae reviewed by Quine (Ref. 28).

V. Antenna Feed System

The transmission system then terminates in an over-moded feed which will create a suitable radiation pattern for illuminating the Cassegrain subreflector. As was mentioned earlier, the 1.75" diameter waveguide provides essentially the correct aperture size for optimally illuminating the Cassegrain system; hence a flare angle horn is not necessary. However, equalization of the E and H plane radiation patterns is required for optimum overall antenna efficiency (Ref. 29). The overmoded corrugated feed section is shown in Fig. 17. The incident TE_{11} mode is transformed into the balanced HE_{11} mode along the feed section via a number of corrugations of varying depth. The balanced HE_{11} mode possesses a circularly symmetric radiation pattern with theoretically no cross-polarization. Similar feeds have been developed for use with linearly polarized plasma heating systems (Refs. 30 and 31). Detailed analysis of the corrugated section is performed using the mode matching and scattering matrix approach of James (Ref. 32). The analysis allows the determination of the number of corrugations and the required depth profile to give the optimum $TE_{11} - HE_{11}$ conversion. The analysis also predicts the resultant feed radiation pattern for an arbitrary set of input modes, i.e., TE_{11} plus any remaining spurious modes. This resultant feed pattern is then used to predict the overall antenna pattern sensitivity, in terms of gain, spillover, and cross polarization, with respect to spurious inputs to the feed. Corrugated feeds typically operate over a much wider bandwidth than that required for this application; therefore such a corrugated section should be capable of producing a suitable radiation pattern over the modest bandwidth of 0.1%.

VI. Discussions and Conclusion

In assessing the state of the art, the development of a 400 kW CW 34 GHz gyroklystron including the overmoded transmission system is subject to technical risks in several areas:

(1) Maintaining RF stability (preventing oscillation). The most challenging technical task is to configure and test an rf circuit which provides adequate gain and efficiency without allowing rf instabilities to occur in any portion of the rf structure. The preferred circuit design for preventing oscillations will include TE_{11} buncher cavities, rf cavity loss, mechanical tunability for the bunchers, cutoff drift tubes and an axial magnetic field profile which can be tailored to help prevent oscillations. Back up circuit design includes a TE_{01} mode buncher section.

(2) Achieving acceptable beam quality. The second most difficult problem is generating a one megawatt beam with adequate beam quality ($\Delta V_{11}/V_{11} \leqslant 5\%$). The beam optics configuration comprising the Pierce gun/wiggler is capable, on paper, of meeting the requirement and has other advantages as well, including space charge limited (low noise) operation. However, a magnetic injection gun (MIG), which has allowed oscillators to achieve efficiencies of over 50%, will be considered as a back-up.

(3) CW window with 400 kW rating. Double disc window technology demonstrated at 28 GHz has already come close to handling the 400 kW CW power level required for the JPL device. Nevertheless a back up approach of a "double-dish" window will also be considered. In this configuration the discs are dish-shaped and are arranged with their convex surfaces in contact with the fluorocarbon cooling channel. The dish shape allows much higher coolant pressure and coolant flow velocities and would therefore be capable of higher CW power levels.

(4) Mode filter. Most of the potential problems associated with the transmission system involve the mode filter and model purity requirement. Resistive wall filters which pass the TE_{on} modes are presently used with gyrotrons. However, such filters do not include a helical winding. Two problems associated with the TE_{11} filter and specifically its helical winding are a very stringent requirement for the tolerance of the pitch of the helical winding (in order to avoid significant attenuation of the TE_{11} mode), and the possibility of breakdown near the windings when transmitting the 400 kW CW power. Also, the modal purity requirement may dictate an excessive length for the mode filter, and a compromise between modal purity and filter length may need to be made.

(5) Antenna feed. With regard to the overmoded feed, corrugated sections have been used to obtain the more desirable HE_{11} radiation pattern from the TE_{11} mode in plasma heating experiments. However, the primary difference between the plasma heating application and the JPL application is the more stringent requirement for the feed radiation pattern which translates into stringent requirements for the modal purity. Due to the large waveguide diameter, an acceptable return loss should be obtainable over the very modest 0.1% bandwidth. Two problems dealing with the feed's response to spurious input modes are intimately related to the problem of the allowable spurious mode level and corresponding mode filter length. Spurious inputs will have an effect on the circular symmetry of the feed radiation pattern, and hence may cause a reduction in the overall efficiency of the Cassegrain

system. Secondly, spurious modes may increase the level of cross polarized radiation in the feed pattern and consequently in the overall antenna pattern.

(6) Power splitter. Finally, should the antenna structure upgrade be insufficient for high efficiency 34 GHz operation due to gravity deformation, a microwave solution using an array of properly phased feeds may be needed to compensate for these effects. The primary difficulty in the design of such a system would be developing a suitable power splitting device. One possible candidate would be a multiple arm coupler designed using tight coupling theory (Ref. 24). Due to significant losses in the dominant waveguide, these runs would need to be made as short as possible.

These then are the technical risks and developments needed in several areas of the K_a-band transmitter. A conceptual design for a 400 kW CW 34 GHz transmitter including overmoded microwave plumbing and an overmoded feed system has been presented. Upon completion of the future final paper design, hardware and implementation stages of the project, the K_a-band transmitter should prove to be a valuable instrument for planetary radar and also serve as a proving ground for new technology which will be transferable to future spacecraft uplinks.

References

1. M. S. Reid et al., "Low-Noise Microwave Receiving Systems in a Worldwide Network of Large Antennas," Proc. IEEE, Vol. 61, pp. 1330-1335, September 1973.
2. S. A. Hovanessian, *Radar Detection and Tracking Systems*, Artech House, Dedham, Massachusetts, Chapter 11, Section 5, pp. 11-22, 1973.
3. M. R. Barnett et al., "An Inverter Powered One Megawatt Power Amplifier for a Radar Transmitter," Proceedings from International Conference on RADAR, RADAR 77, London, England, pp. 349-363, October 1977.
4. D. D. P. King, "Millimeter-Wave Prospectus," Microwave Journal, Vol. 10, pp. 24-29, November 1967.
5. J. L. Hirshfield, "Gyrotron," in *Infrared and Millimeter Waves,* Vol. 1, Academic Press, New York, pp. 1-54, 1979.
6. V. L. Granatstein and S. Y. Park, "Survey of Recent Gyrotron Developments," Proceedings of the International Electronics Devices Meeting (IEDM), Washington, D.C., pp. 263-266, December 1983.
7. R. Symons, H. Jory, S. Heggi, and P. Ferguson, "An Experimental Gyro TWT," IEEE Trans. Microwave Theory Tech., Vol. MTT-29, pp. 181-184, March 1981.
8. P. Ferguson, G. Valier, and R. Symons, "Gyrotron-TWT Operating Characteristics," IEEE Trans. Microwave Theory Tech., Vol. MTT-29, pp. 794-799, August 1981.
9. L. A. Barnett et al., "An Experimental Wide-Band Gyrotron Traveling-Wave Amplifier," IEEE Trans. Electron Device, ED-28, pp. 872-875.
10. A. Arfin and A. K. Ganguly, "A Three-Cavity Gyroklystron Amplifier Experiment," Int. J. Elect., Vol. 53, No. 6, 709-714, 1982.
11. S. Hegji, H. Jory, and J. Shively, "Development Program for a 200 kW CW 28 GHz Gyroklystron," Varian Associates, Inc., Internal Document.
12. D. Stone, M. Chodorow, and A. Nordquist, "Fast Wave Amplifiers for Space Communications Phase II: Gyroklystron Design Study," Final Report, prepared by Varian Associates, Inc., for the NASA Lewis Research Center, April-September 1982.

13. M. Caplan, "Gain Characteristics of Stagger Tuned Multicavity Gyroklystron Amplifiers," IEEE International Conference on Infrared and Millimeter Waves, Miami Beach, Florida, Session W4.2, December 1983.

14. K. Felch, R. Bier, M. Caplan, and H. Jory, "100 GHz, 1 MW CW Gyrotron Study Program," Final Report, prepared by Varian Associates, Inc., under subcontract P.O. #53Y-21453C, for the Oak Ridge National Laboratory, Nashville, Tennessee, operated by Union Carbide Corp. for the U.S. Department of Energy, under contract #W-7405-eng-26.

15. C. Moeller, "Mode Converters Used in Doublet III ECH Microwave System," Int. J. Elect., Vol. 53, No. 6, pp. 573-585, 1982.

16. F. Sporleder and H. G. Unger, *Waveguide Tapers, Transitions and Couplers,* Institute of Electrical Engineers, London, England, Chapter 2, 1979.

17. H. Jory et al., "First 200 kW CW Operation of a 60 GHz Gyrotron," IEDM Technical Digest, Washington, D.C., pp. 267-270, December 1983.

18. K. R. Spangeberg, *Fundamentals of Electron Devices,* McGraw Hill, New York, pp. 427-428 and 464-465, 1957.

19. K. H. Sann, "The Measurement of Near-Carrier Noise in Microwave Amplifiers," IEEE Trans. Microwave Theory Tech., Vol. MTT-16, No. 9, pp. 761-766, September 1968.

20. H. Hashimoto et al., "A 30 GHz 40 Watt Helix Traveling-Wave Tube," Proc. IEDM, Washington, D.C., pp. 133-136, December 1983.

21. J. J. G. McCue and E. A. Crocker, "A Millimeter-Wave Lunar Radar," Microwave Journal, pp. 59-63, November 1968.

22. M. H. Cohen, *Superconductivity in Science and Technology,* Univ. of Chicago Press, Chicago, Illinois, p. 103, 1968.

23. H. T. Coffey, K. R. Efferson, and G. J. Svenconis, "A Study of the Requirements for Shipboard Use of Superconducting Magnet Systems Used for Gyrotrons," Naval Research Laboratory, Washington, D.C., Contract No. N00014-81-C-2586, American Magnetics, Inc., June 1982.

24. S. E. Miller, "Coupled Wave Theory and Waveguide Applications," Bell System Technical Journal, Vol. 33, pp. 661-719, 1954.

25. K. Felch, R. Bier, L. Fox, H. Huey, H. Jory, J. Manca, J. Shively, S. Spang, and C. Moeller, "Analysis of the Output Mode from 60 GHz, 200 kW Pulsed and CW Gyrotrons," IEEE International Conference on Infrared and Millimeter Waves, Miami Beach, Florida, Session T4.2, December 1983.

26. G. Janzen and H. Stickel, "Mode Selective Directional Couplers in Overmoded Circular Waveguides," IEEE International Conference on Infrared and Millimeter Waves, Miami Beach, Florida, Session TH4.6, December 1983.

27. S. P. Morgan and J. A. Young, "Helix Waveguide," Bell System Technical Journal, pp. 1347-1384, November 1956.

28. J. P. Quine, "Oversize Tubular Metallic Waveguides," in *Microwave Power Engineering,* Academic Press, New York, pp. 178-212, 1968.

29. P. D. Potter and A. Ludwig, "Antennas for Space Communications," JPL Space Programs Summary No. 37-26, Vol. IV, pp. 200-208, April 30, 1964.

30. M. Thumm, G. Janzen, G. Muller, P. G. Schuller, and R. Wilhelm, "Conversion of Gyrotron TE_{on}-Mode Mixtures into a Linearly Polarized HE_{11} Wave," IEEE International Conference on Infrared and Millimeter Waves, Miami Beach, Florida, Session TH4.7, December 1983.

31. J. L. Doane, "Mode Converters for Generating the HE_{11} (Gaussian-like) Mode from TE_{01} in Circular Waveguide," Int. J. Elect., Vol. 53, pp. 573-585, December 1982.

32. G. L. James, "Analysis and Design of TE_{11} to HE_{11}, Corrugated Cylindrical Waveguide Mode Converters," IEEE Trans. Microwave Theory Tech., Vol. MTT-29, pp. 1059-1066, October 1981.

Table 1. K_a-band transmitter specifications

Frequency	34 GHz
Bandwidth	0.1%
RF power output	400 kW CW (+ 86 dBm)
RF stability	0.1 dB over 1 transmit cycle
Incidental AM	60 dB below carrier at all modulating frequencies above 1 Hz
Phase stability	1.0×10^{-15} (1000 seconds) with goal of 1.0×10^{-16} (1000 sec)
Incidental PM (jitter)	$< 1°$ peak to peak
Noise figure	-80 dB/MHz
Transmit pulse	20 sec minimum to a few hours maximum
Modulation	*Phase Modulation*: 0-100% carrier suppression 1 kHz to 2 MHz. This is accomplished by PN code modulation of length 2^n-1 where n = 6 to 15 and at baud length of 0.5 sec to 1000 sec.
	FSK: Shifting carrier frequencies separated from 1 Hz to 1 MHz and switching in less than 1 msec every 30 seconds.

Table 2. JPL gyroklystron specifications

f_0:	34 GHz
Bandwidth:	0.1% (1 dB points)
Output power:	400 kW CW saturated (goal)
Output mode:	Dominant $TE_{11}°$ circularly polarized mode with very high modal purity (-30 dB for each extraneous mode) and circular polarization within 1 dB
Noise figure:	-80 dB/MHz
Orientation:	Gyroklystron and auxiliary components such as its magnets must be capable of operating through 75° of elevation motion (zenith to 15° above horizon) and simultaneously through 360° in azimuth when installed on the antenna
Efficiency:	40% (goal)
Saturated gain:	50 dB minimum (goal)

Table 3. Gyroklystron circuit design

a. Characteristics

Characteristic	Value
Voltage	80 kV
Current	12.5 amps
Beam radius	0.120 cm
Perpendicular velocity/parallel velocity	1.5
Magnetic field	12.5 kgauss
Number of cavities	4
Total length	7.84 cm
Input coupling Q_{coupl}	299
Output external Q_{ext}	120
Mode buncher cavities	TE_{111}
Mode output cavity	TE_{121}
Small signal gain	57 dB
Saturated gain	50 dB
Saturated efficiency	46.5%
Saturated bandwidth (-1 dB points)	0.3%

b. Cavity configuration

Cavity number	Length (cm)	Radius (cm)	Resonant frequency (GHz)	Cold Q_o	Beam Q_B
1	0.784	0.314	33.9	299	330
2	0.784	0.317	33.7	400	330
3	0.784	0.318	33.6	400	330
4	1.725	0.769	34.2	120	-220

c. Drift tubes

Drift tubes	Length (cm)
1	0.784
2	0.784
3	2.196

Table 4. Spurious mode level at converter output of mode converter TE_{12}–TE_{11} (99% efficient)

Spurious modes produced	Levels produced
TE_{13}	-27 dBc
TE_{14}	-34 dBc
TM_{11}	-38 dBc
TM_{12}	-23 dBc
TM_{13}	-37 dBc
TM_{14}	-35 dBc

Table 5. AM pushing factors

Parameter	dB/%
Cathode voltage	0.5 dB/%
Main magnet coil current	0.5 dB/%
Load VSWR	1.6 dB for VSWR 2:1 (oscillation at VSWR 2.4:1)
RF drive (input power)	0.007 dB/%
Filament voltage	0.005 dB/% (typical)
Wiggler coil current	0.6 dB/% (typical)
Gun coil current	0.5 dB/% (typical)

Table 6. PM pushing factors

Parameter	°/%
Cathod voltage	6.4°/%
Main magnet coil current	100°/%
Load VSWR	TBC[a]
RF drive (input power)	TBC
Filament voltage	TBC
Inlet coolant temperature	TBC
Wiggler coil current	TBC
Gun coil current	TBC

[a]To be calculated

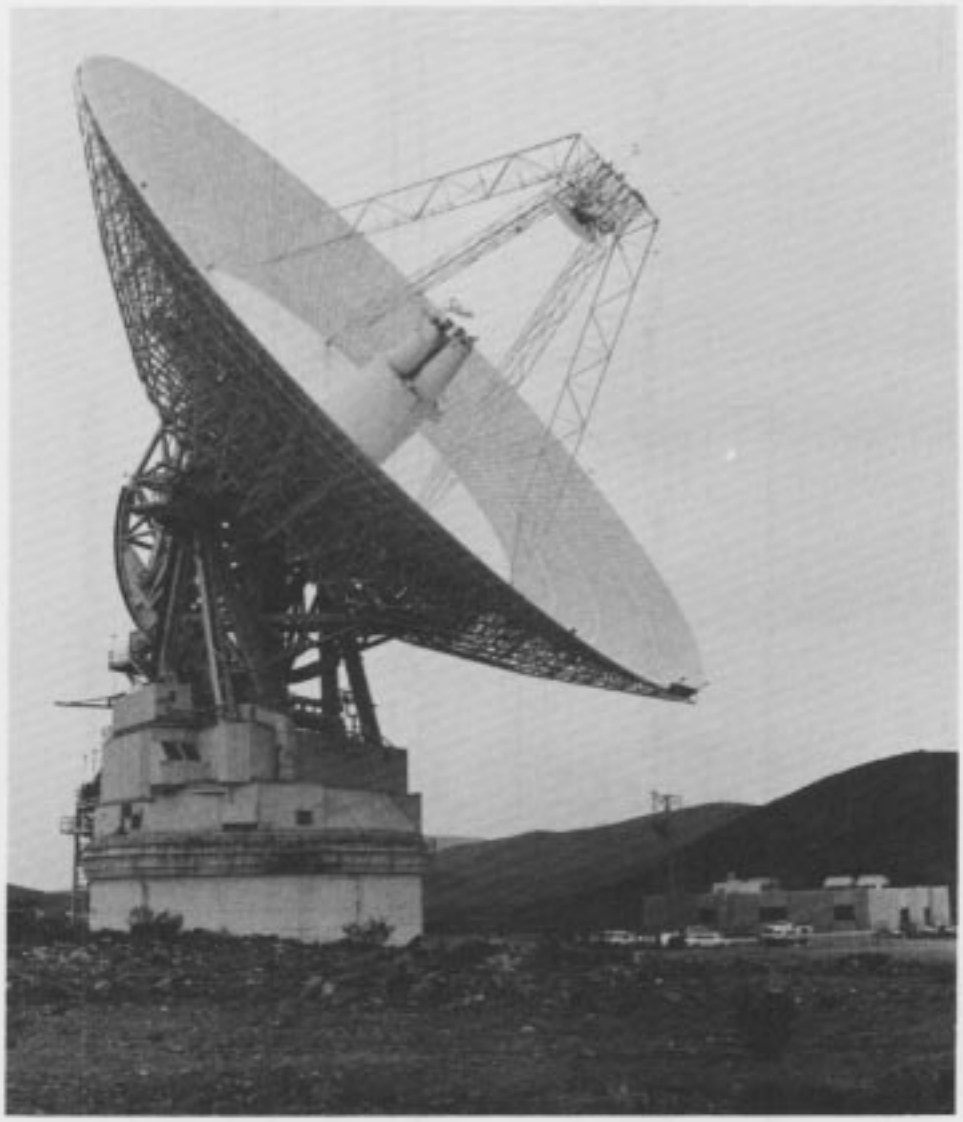

Fig. 1. 64 meter diameter antenna at Goldstone, California

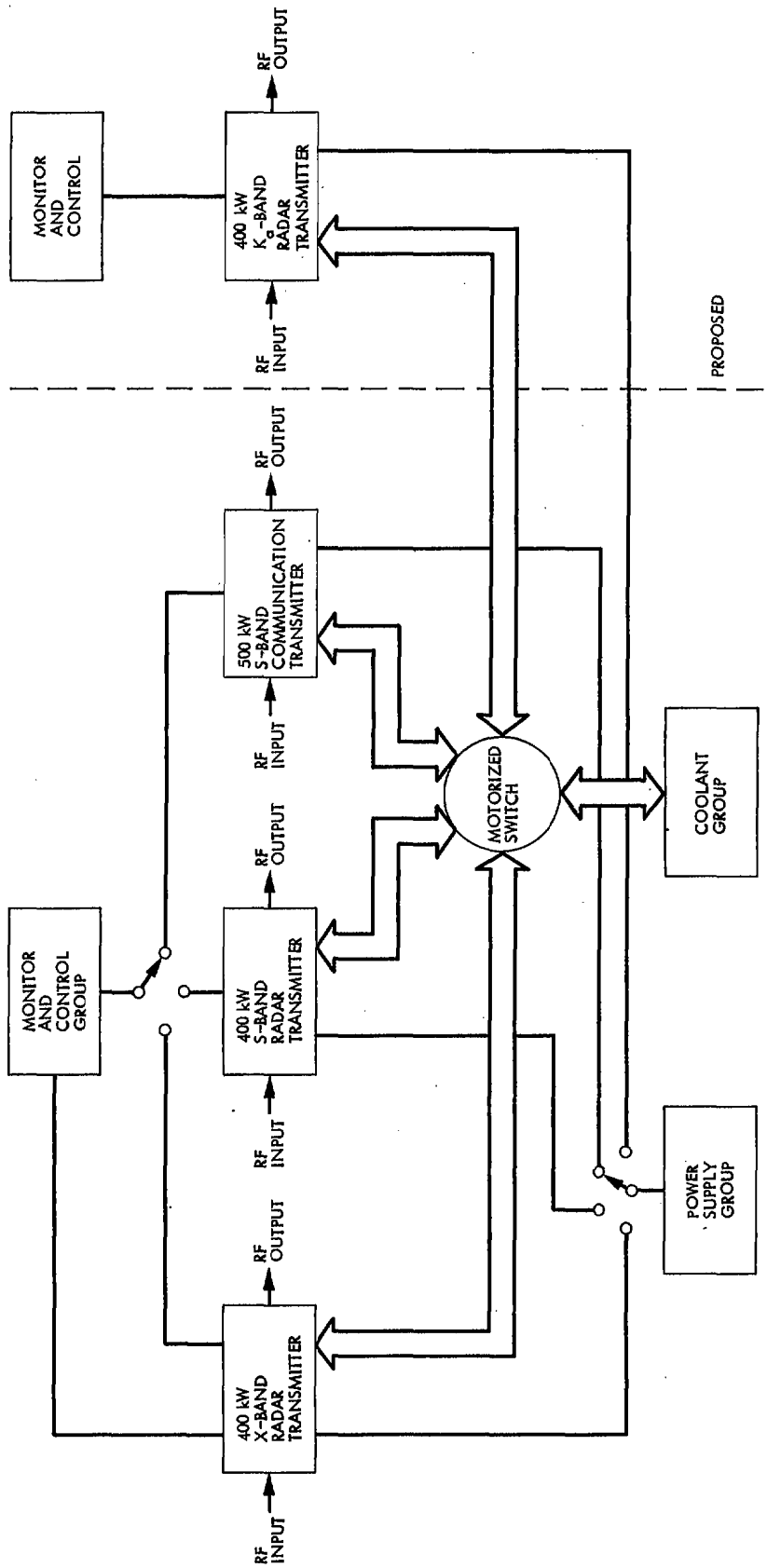

Fig. 2. Transmitters on the 64 meter antenna

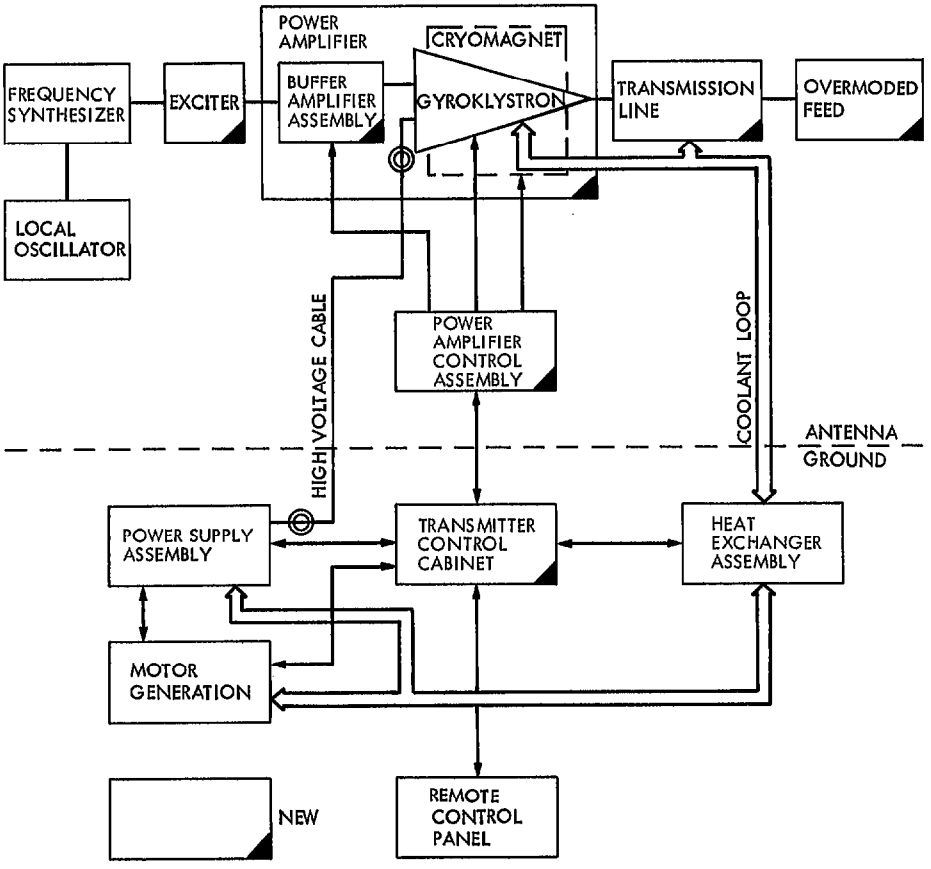

Fig. 3. K_a-band transmitter block diagram

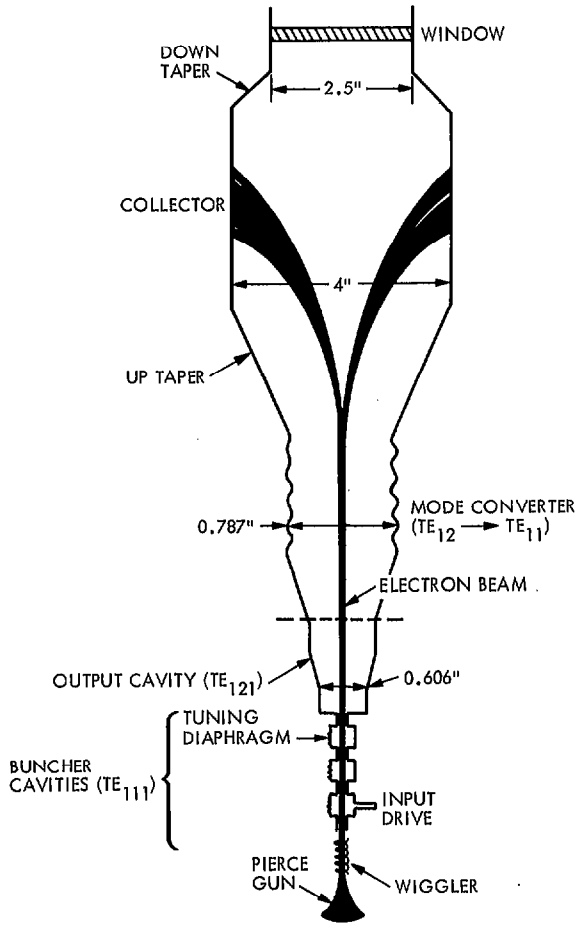

Fig. 4. Proposed 35 GHz gyroklystron schematic diagram

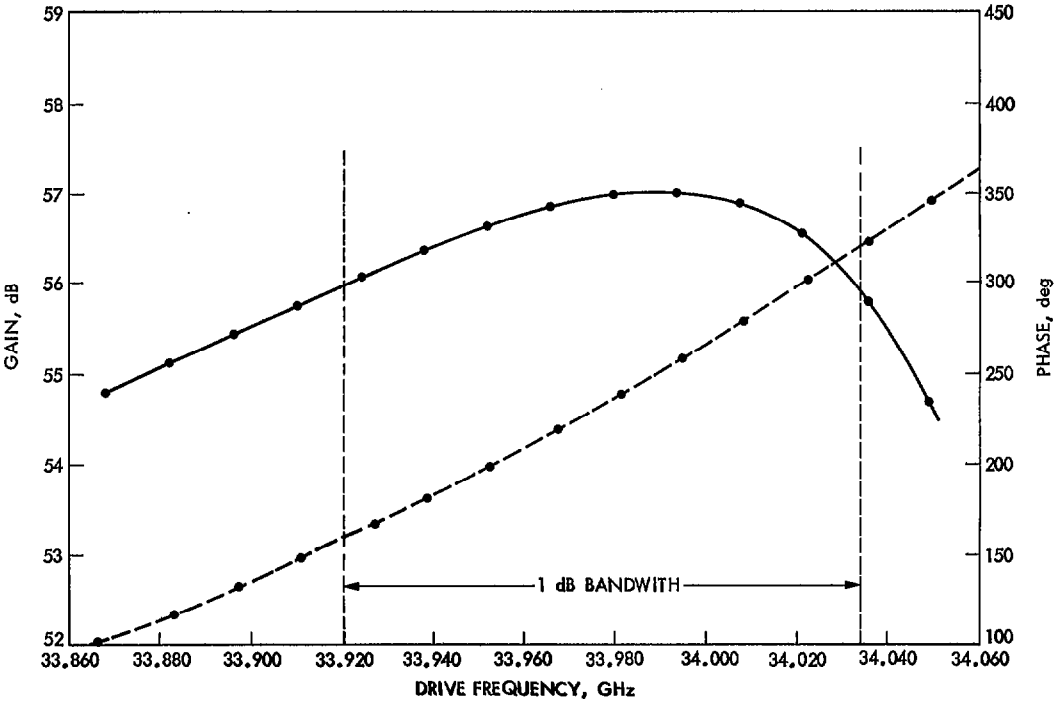

Fig. 5. Linear gain vs. frequency, and phase vs. frequency of the proposed 34 GHz gyroklystron

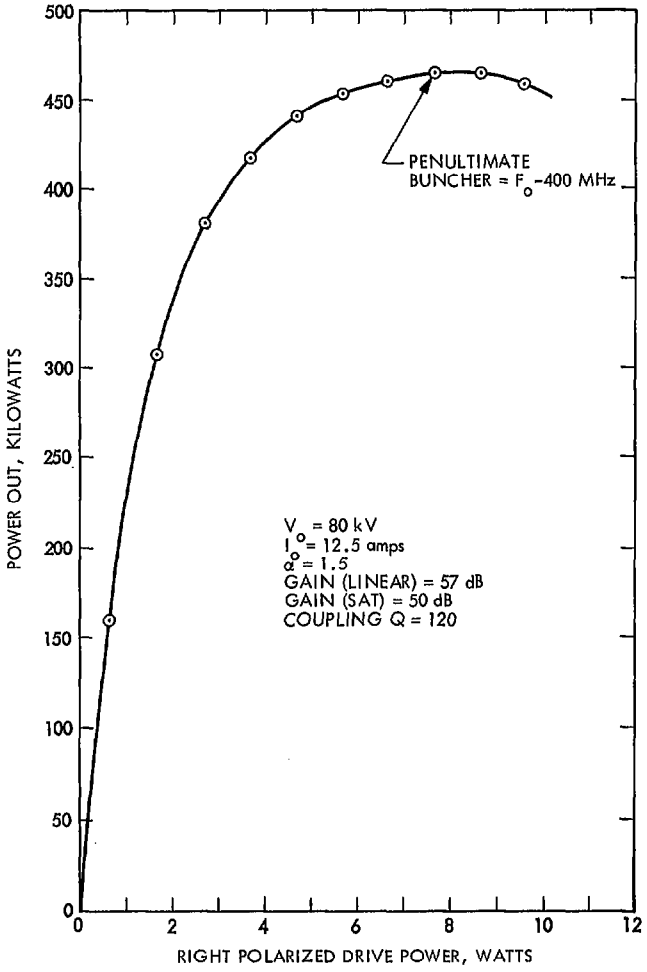

Fig. 6. Power out vs. drive power for the proposed 34 GHz gyroklystron

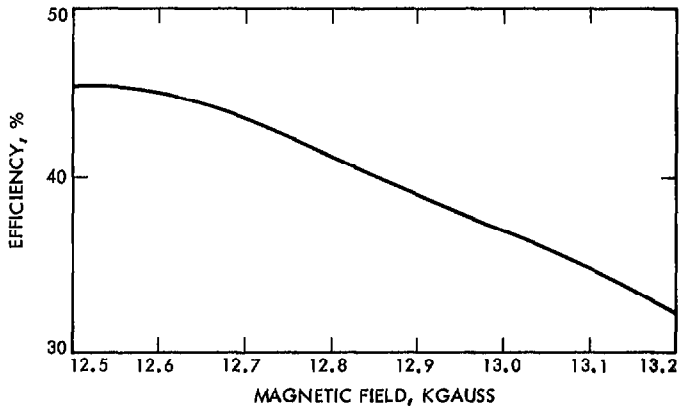

Fig. 7. Efficiency as a function of magnetic field for the 34 GHz gyroklystron

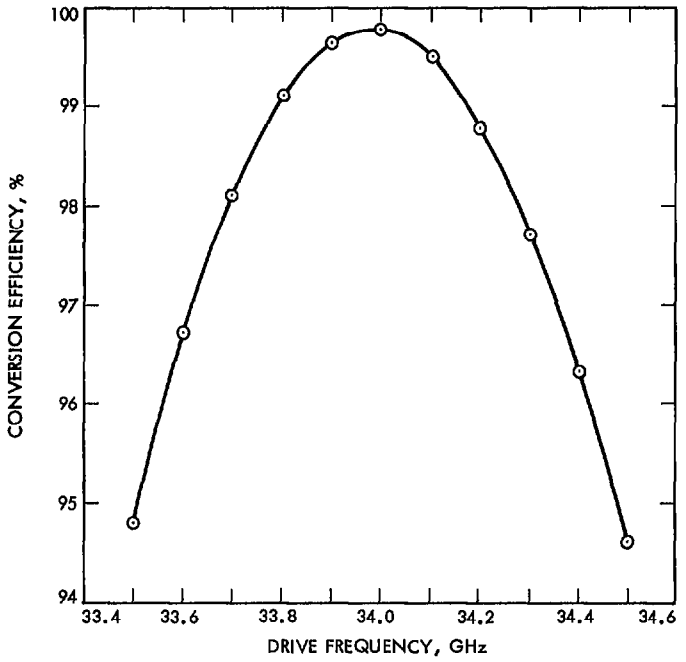

Fig. 8. Calculated conversion efficiency vs. drive frequency of the TE_{12} to TE_{11} converter

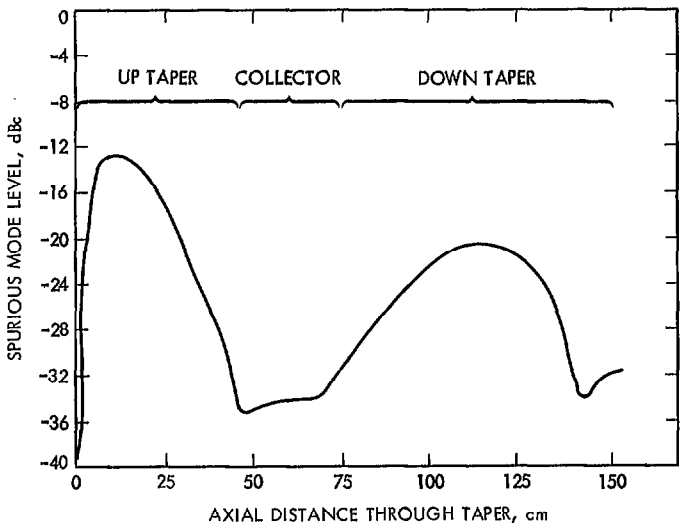

Fig. 9. Spurious TE_{1n} mode level in an optimized TE_{11} compound-tapered collector vs. axial distance. The final spurious mode level at the output is −32 dBc.

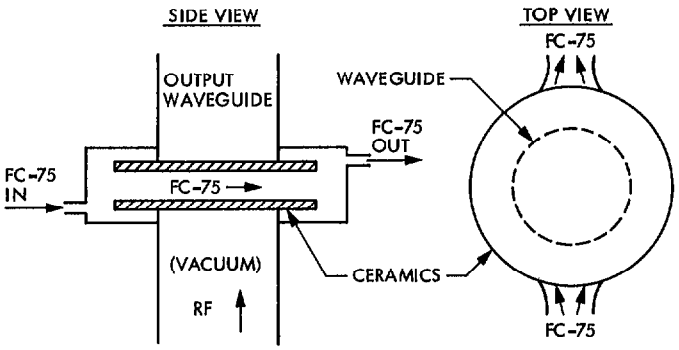

Fig. 10. Schematic diagram of a double disc window

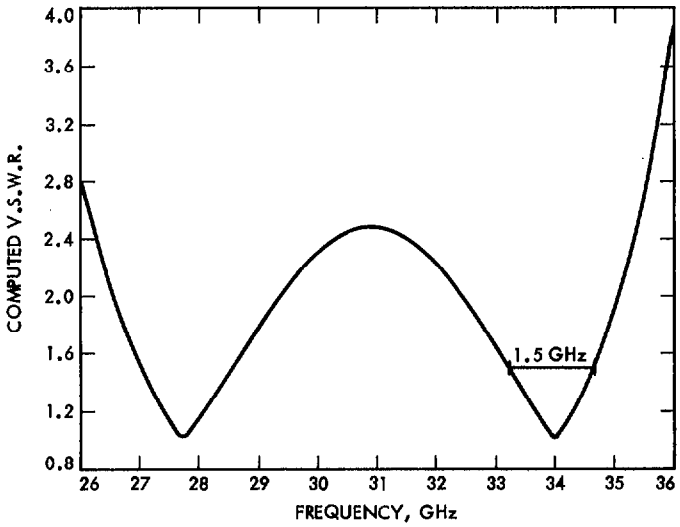

Fig. 11. Computed VSWR for a 34 GHz double disk window

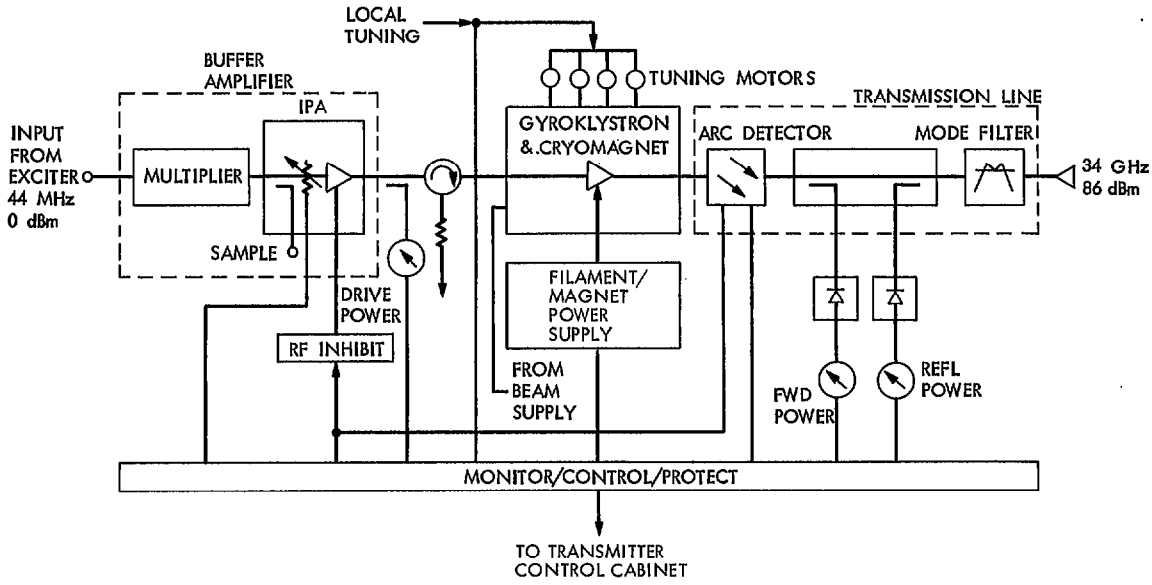

Fig. 12. Power amplifier block diagram

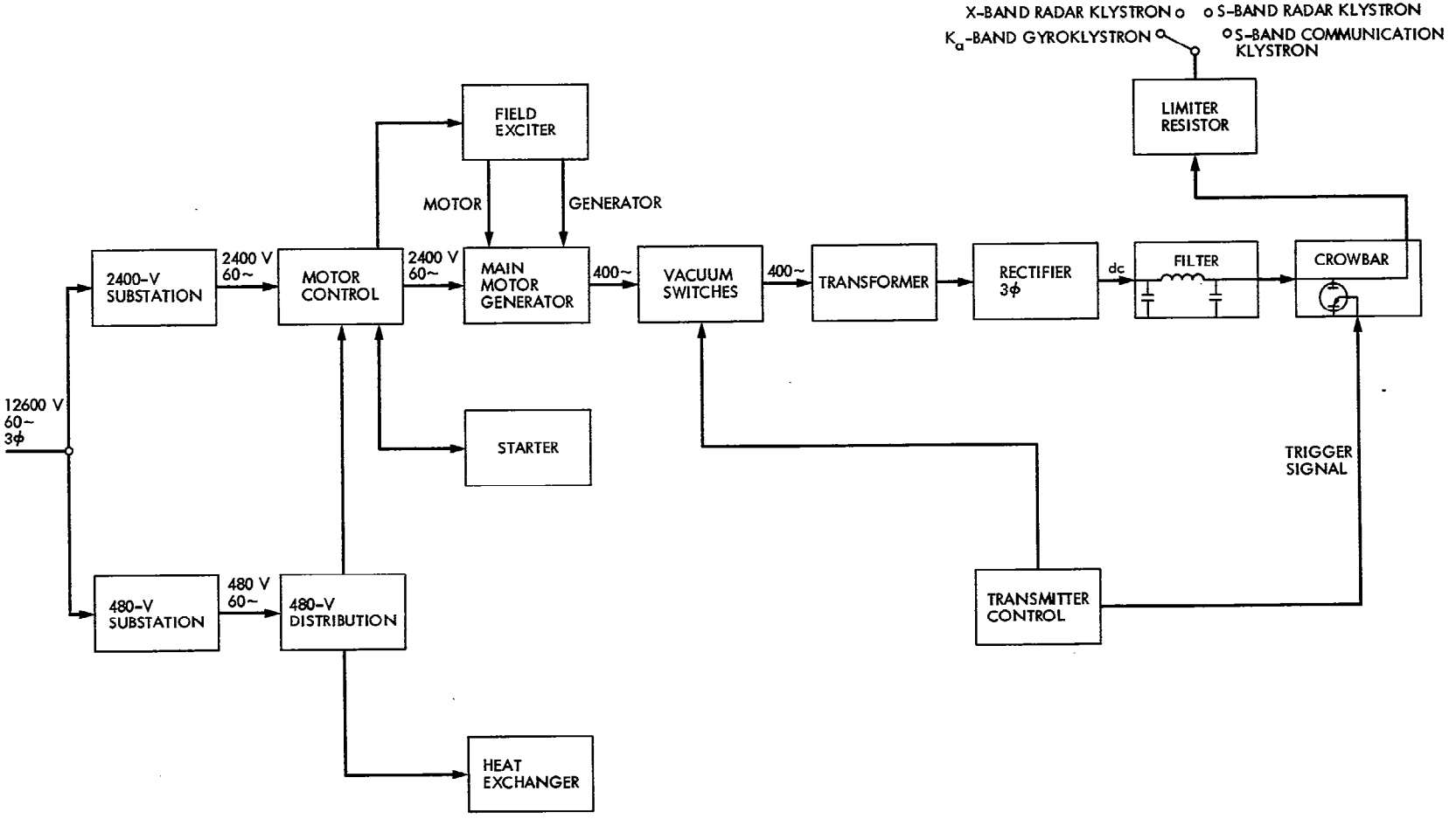

Fig. 13. Power supply block diagram

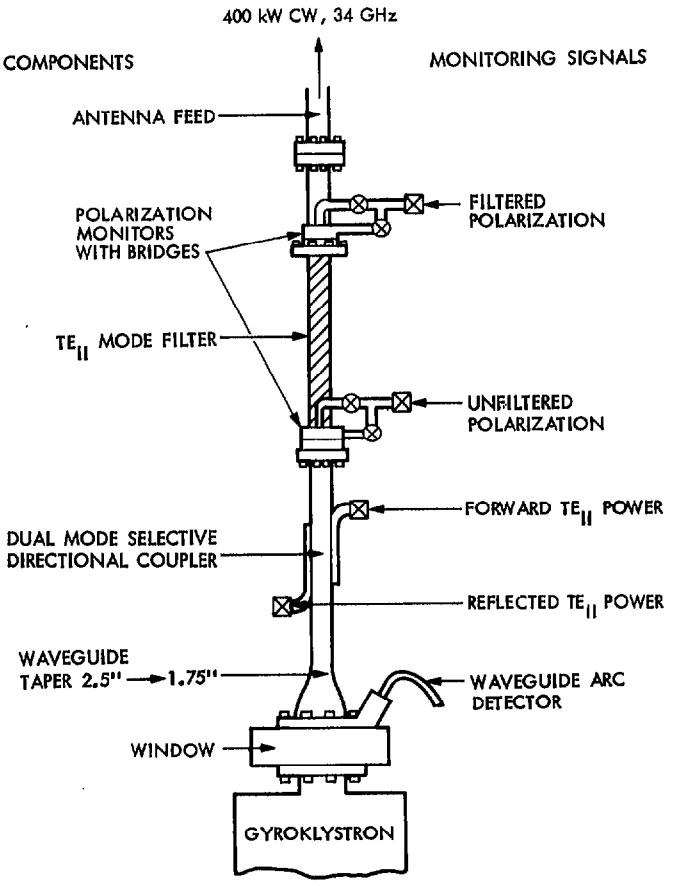

Fig. 14. Proposed 1.75 in. diameter 400 kW CW TE_{11} transmission line system

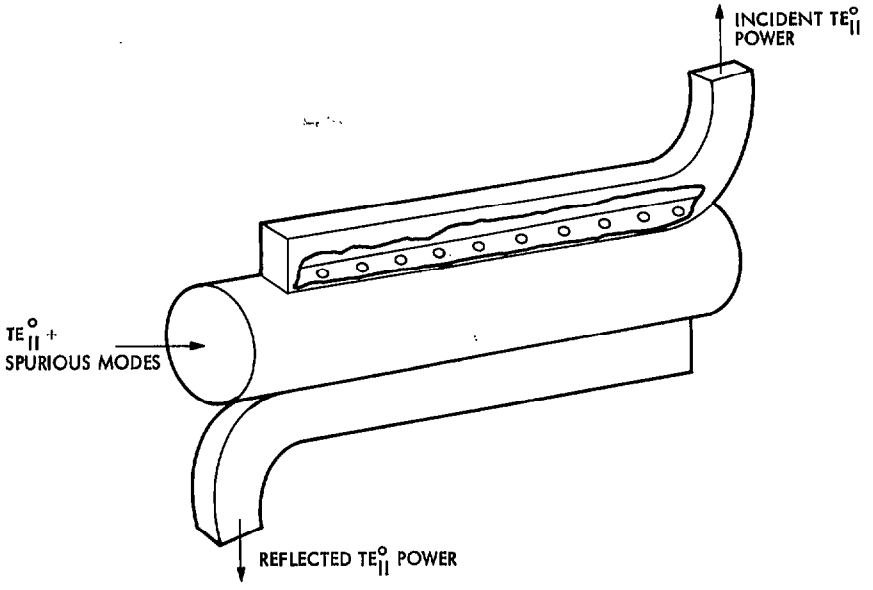

Fig. 15. A dual mode selective directional coupler

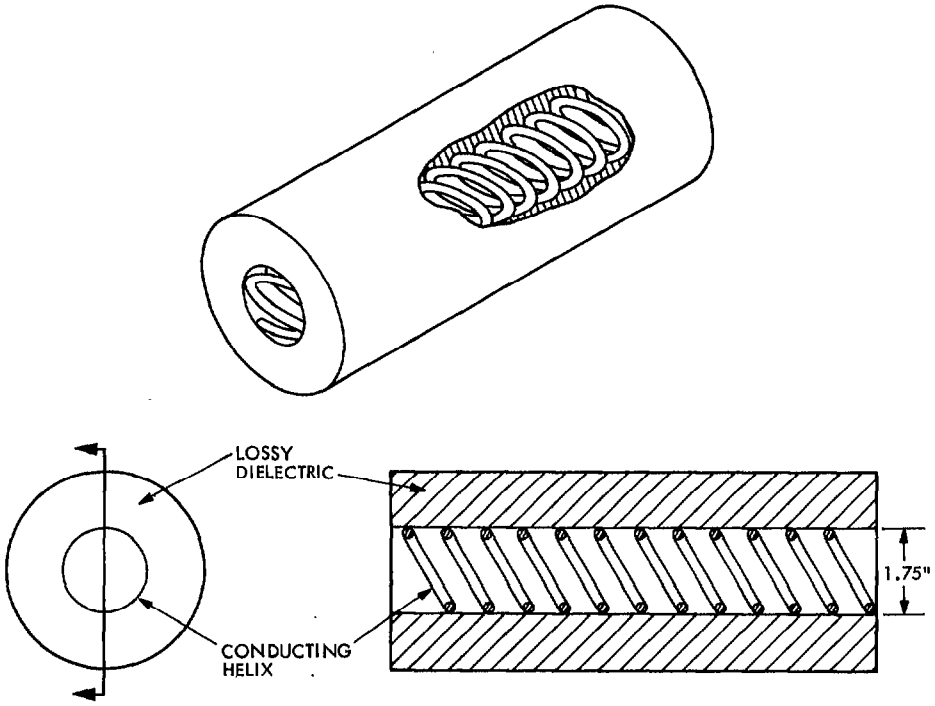

Fig. 16. The TE_{11} mode filter

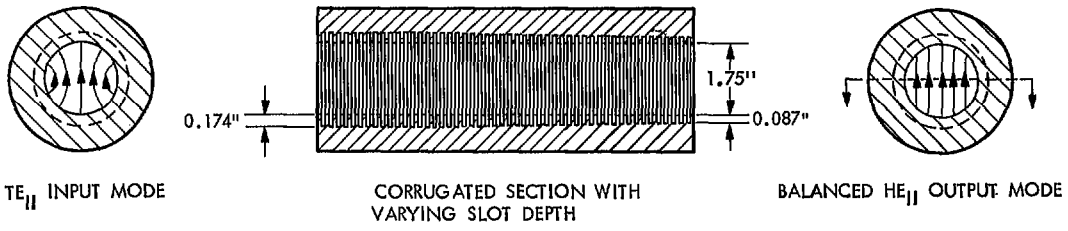

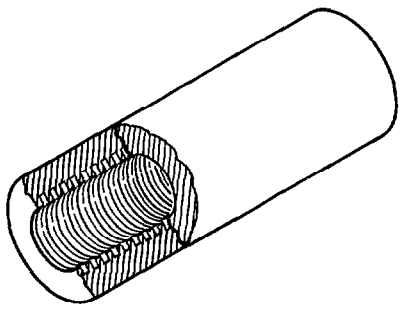

Fig. 17. The antenna feed